PRZEGLĄD SPAWALNICTWA
Welding
TECHNOLOGY REVIEW

DOI: http://dx.doi.org/10.26628/wtr.v91i8.1046

Article

The effect of the current pulsation frequency on heat supply results during pulsed current TIG welding in 301L stainless steel

Małgorzata Ostromęcka[1,*], Andrzej Kolasa[2]

[1] Railway Research Institute, Poland
[2] Warsaw University of Technology, Poland
Prof. Andrzej Kolasa; a.kolasa@wip.pw.edu.pl
* Correspondence: Małgorzata Ostromęcka, Ph.D.; malgorzata@ostromecka.pl

Received: 30.04.2019; Accepted: 02.09.2019

Abstract: The paper presents the influence of pulsation frequency on the results of pulsed current TIG welding based on two criteria: geometric parameters of weld and changes in microstructure. The investigations were carried out for 301L austenitic stainless steel with constant current parameters, constant welding speed, 50% duty cycle ratio and constant heat input. The results were referred to the commonly used methods for measuring the amount of heat input.

Keywords: TIG welding; pulsed current; heat input; pulsation frequency

Introduction

TIG pulsed welding has been known for over 50 years. Main objective of the development of this method was to minimize the heat introduced into the welded material so that the process could be mechanized or automated while providing the desired joint properties. Initially, this method found few applications, but with the development of welding power sources, it began to appear in various production areas. Currently, TIG pulsed welding is used in the production of heat exchangers, boilers at nuclear power plants and chemical plants, in classical power engineering, in orbital pipe welding and in industries related to high quality requirements, e.g. in aviation. However, the availability of the method is much greater and welding companies offers increasingly TIG welding equipment with the "pulse"option.

The use of pulsed current in TIG welding is strictly connected to the frequency of pulsation as one of the main process parameters. Unfortunately, its impact on the final welding result is not sufficiently studied. It is well known that an increase in frequency causes the arc to "stiffen" and in many cases is associated with the possibility of affecting the depth of penetration. However, this relationship is not obvious and there are no scientific publications on this topic.

In recent years, pulsed current TIG welding a is carried out in two variants depending on the frequency of pulsations. Pulsed current in the low frequency range from 0.1 to 10 Hz and current with very high pulsation frequency above 1 kHz are used. Some studies [1] report that at frequencies above 6 Hz there is no special difference between the pool temperature during the pulse and the base, which brings this process closer to DC welding, making it in the opinion of some researchers not very interesting from the scientific point of view. In contrast, high-frequency pulsation causes an increase in arc pressure, affecting the penetration depth. Recently, some research has been devoted to welding in the ultra-high frequency range, i.e. 20÷80 kHz [2÷4].

The frequency of pulsation during TIG welding is one of the basic parameters of the process, however, it is not associated with any defined relationship with the welding heat input, which in turn is considered one of the universal technological parameters. Moreover, welding with current pulsation at the same heat input (calculated in accordance with the formula given in the standards), when changing the frequency of pulsations, results in the formation of joints with different geometric parameters.

Observations of Arivarasu M. et al. [5] showed that with high frequency pulsed welding, full penetration can be achieved at lower heat input values.

Traidia [6] created a model of the TIG welding process, in which he compared the conditions of welding with pulsed and constant current. He determined that with the same heat input different volumes of the liquid metal pool can be obtained for pulsed and constant current. He also pointed out that in order to

produce a weld with the same geometry as for given pulsed current parameters, the welding current should be increased, which will significantly increase the heat input. At the same time, with the same average welding current, different sizes of the weld pool can be obtained, depending on the difference between the pulse current and the base current level. Similar observations were presented in the study [7] and, it was noticed also that when the current coefficient changes, the average current value may remain constant but the effective current value changes.

Ugla [8,9] noted that during high frequency welding, the dendrite arms break in the weld during solidification, which in turn promotes the formation of a more homogeneous structure and improves the mechanical properties of the joint.

Observation of the impact of pulsating current frequency changes on the results of TIG welding can give the opportunity to determine whether the welding pool formation mechanism is changing and whether the change in frequency affects the amount of heat introduced into the material.

Currently, more and more controversy arise in the scientific community regarding the issue of heat input [10÷12], in particular in relation to impulse processes. Mostly, the problem is reduced to the measurement and calculation aspects only. Between the standard PN EN 1011-1 (Welding – Recommendations for metal welding – Part 1: General guidelines for arc welding) and the American ASME IX QW-409 (Welding Procedure and Performance Qualification Electrical Characteristics) there are significant differences in the approach to heat input measuring issues. Thus, the study of the impact of the frequency of pulsed current during TIG welding can verify the usefulness of heat input as a parameter determining the amount of heat input per unit of weld

Materials and research methodology

The chemical composition of steel was determined using an emission spectrometer. The results of the analysis are presented in table I.

Table I. Chemical composition of the tested material

C	Si	Mn	P	S	Cr	Mo	Ni	V	Ti	Nb	Cu	Co	W	N
0.019	0.48	1.48	0.026	0.015	18.14	0.148	6.31	0.029	0.010	0.012	0.13	0.175	0.059	<0.04

The material composition corresponds to 301L grades according to ASTM A666-03 or X5CrNi17-7 steel according to PN-EN 10088-2:2014-2.

Samples of 100x100x3 mm were fixed on a copper back plate. Due to the possibility of precise setting of welding current pulsation parameters, Fronius TIG MagicWave 2500 DC power was used. The torch with the 2,4 mm 1,5% lanthanated tungsten electrode was mounted on the line positioner. The process was performed with any filler material. As a shielding gas pure argon (9,8 l/min. flow) was used.

The measurements were performed with the Siglent SDS 1072CML oscilloscope and an intermediary KWR1 measuring cassette containing the necessary current and voltage measuring transducers. The oscilloscope has two independent measuring channels with a range of 70 MHz. The screen displayed voltage waveforms (blue) and current (yellow) as a function of time and measured trueRMS and average values for these parameters as shown in figure 1.

The process was carried out at the same parameters of the pulse current I_p, base current I_b, pulse duty factor r_I, arc voltage U and the welding velocity v. A series of welds was carried out with pulsation frequencies of: 0.5, 1, 1.5, 5, 7.5, 10, 50 and 100 Hz. Using an oscilloscope, the average and effective voltages and intensities were measured for the set waveform parameters (Table II). In all cases, the measurements were identical.

Table II. Parameters of welding of 301L steel samples

Settings			Oscilloscope measurements				Welding speed
I_p [A]	I_b [A]	r_I[%]	I_{av} [A]	I_{RMS} [A]	U_{av} [V]	U_{RMS} [V]	v [mm/s]
140	28	50	88	102	11.6	13,6	2.33

Heat input calculated on the basis of average values of current and arc voltage was calculated according to the formula given in PN EN 1011-1 and was 0.26 kJ/mm assuming a constant value of 0.6 thermal efficiency coefficient. In the case of substitution of RMS current and voltage into the formula, the value of heat input was higher, i.e. 0.36 kJ/mm. It should be emphasized that, regardless of the method used to calculate the heat input (calculated on average or effective parameters), its value was constant and independent of the frequency of current pulsations.

Metallographic specimens were prepared in accordance with standard metallographic procedures. The revealing of 301L steel microstructure was carried out by chemical etching with a reagent known as Mi16Fe with a chemical composition of: 1 part. vol. HNO_3, 2 part vol. HF, 3 pcs. vol. glycerin.

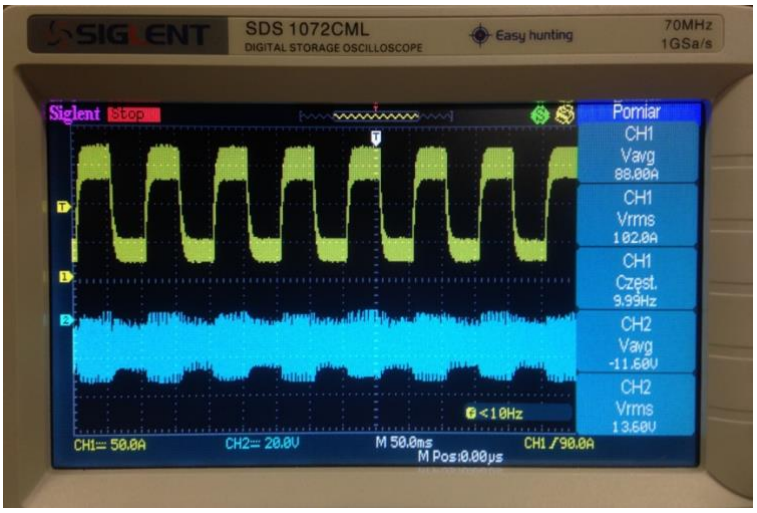

Fig. 1. Screen image of the oscilloscope during pulsed current welding at 10 Hz of 301L material

Surface topography tests were performed on a scanning microscope equipped with a field emission electron gun by JEOL JSM-7600F using a secondary electron detector. Material tests were performed using an Oxford X-MaxN 150 energy dispersion X-ray spectrometer integrated with a scanning microscope.

Observations and test results

Calculations of the welding jump, which in processes carried out above 5 Hz was below 0.5 mm (Table III), suggested that from the frequency of 5 Hz the process was more continuous, i.e. overlapping pools will not be visible in the weld.

Table III. The jump values and pulse duration for a given pulse frequency

f[Hz]	0.5	1	1.5	5	7.5	10	50	100
s[mm]	4.66	2.33	1.55	0.47	0.31	0.23	0.05	0.02
$t_i=t_p$ [s]	1.00	0.50	0.333	0.100	0.067	0.05	0.010	0.005

The recommended technological weld jump for pulsed TIG welding in an argon shield without additional material for 3 mm thick austenitic steel is within 1.5÷2.5 mm [13]. In the case of the welding performed at frequencies of 1 and 1.5 Hz, this condition was met. For the frequency of 0.5 Hz, to meet this condition, it would be necessary to reduce the welding speed and it what would change the arc energy.

Figure 2 shows a comparison of the longitudinal section of welds depending on the frequency of current pulsation. For frequencies from 0.5 to 1.5 Hz, it is easy to indicate separate spot welds and associate them with the thermal cycle and the pulsating current. However, at 50 Hz pulsation frequency, no separate pools can be distinguished in the structure, besides, very long dendrites are visible, whose growth is conditioned by the direction of heat dissipation. The image does not show any cyclic changes in the microstructure. It can therefore be concluded that the change in the frequency of the current pulsation affects the nature of crystallization.

During welding at the low pulsation frequency, the fusion depth as well as the cross-sectional area of the fusion change along its length over each cycle. This is due to the fact that each spot weld has geometry close to half of the cycloid, and therefore its cross-section depends on where the sample was taken (Fig. 3).

Macroscopic studies were aimed at assessing the geometrical aspects of the received fusion. The measurements are summarized in table IV, and the macrographs are shown in figure 4. The results were used to analyze the width and depth of fusion, the shape coefficient and the melting efficiency depending on the frequency of the current pulsations.

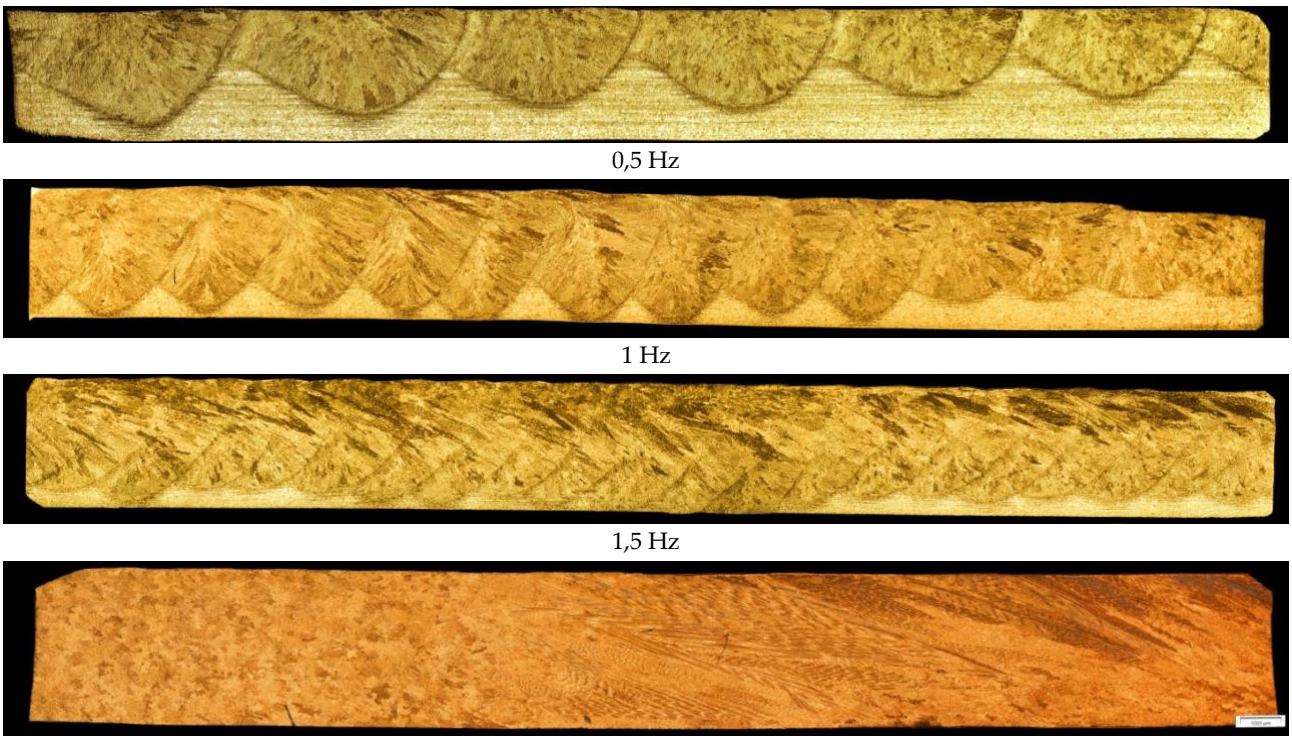

Fig. 2. The longitudinal cross-section of welds made at different frequencies. The length of the section is approx. 30 mm. Each image was merged from 11÷13 photos using Adobe Photoshop. Direction of welding to the left

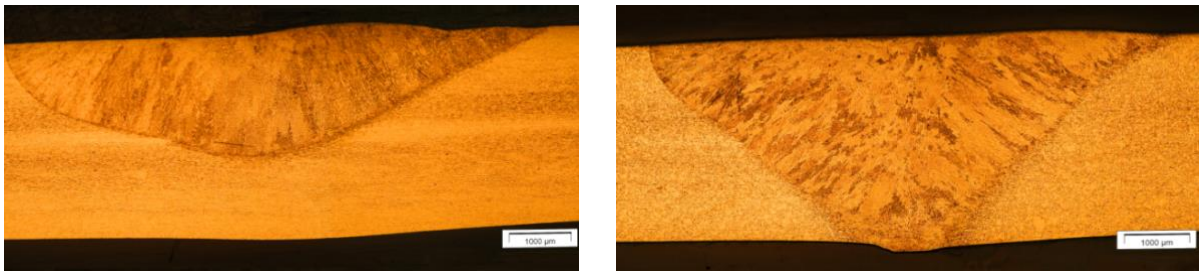

Fig. 3. Comparison of the shape and surface area of cross-sections taken within one cycle for welding at 0.5 Hz

Table IV. Measurements of welds geometry for different pulsation frequencies

No.	f [Hz]	A [mm²]	Width [mm]	Depth [mm]	Shape coefficient φ
1a	0.5	11.60	8.99	2.1	4.28
1b	0.5	16.36	8.36	3.0	2.78
2	1	7.94	5.36	2.85	1.88
3	1.5	10.27	5.62	3.0	1.87
4	5	7.65	5.13	2.65	1.91
5	7.5	6.04	5.06	1.86	2.72
6	10	7.74	5.50	2.15	2.56
7	50	10.01	4.96	3.0	1.65
8	100	11.04	5.77	3.0	1.92

The depth of penetration plays a key role in determining its mechanical strength and dimensioning of welds, therefore the ability to control this parameter is extremely important. When analyzing the obtained results, it must be taken into account that depending on the frequency, we can obtain a variable or constant depth of penetration. In the case of the frequencies used, taking into account the jump values and observations of the longitudinal sections of the welds (Fig. 3), the range of pulsation frequencies from 0.5 to 1.5 Hz was determined as the one in which cyclic differences in melting depth can be expected. Above 5 Hz, the penetration depth could be considered constant. The results obtained are presented on a graph on a logarithmic scale (Fig. 5).

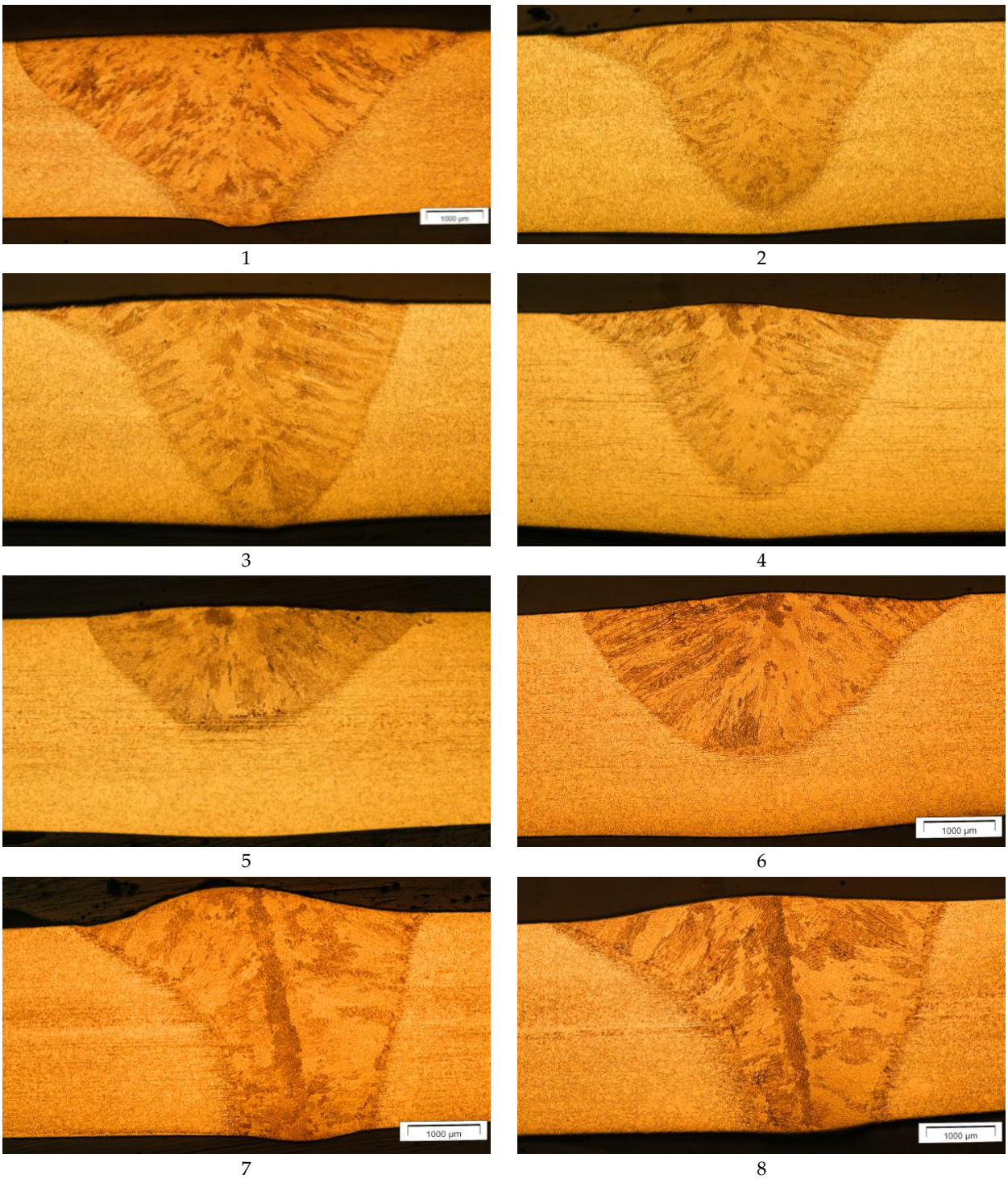

Fig. 4. Macrographic images of welds made at different pulse current frequencies (measurement results are given in Table IV)

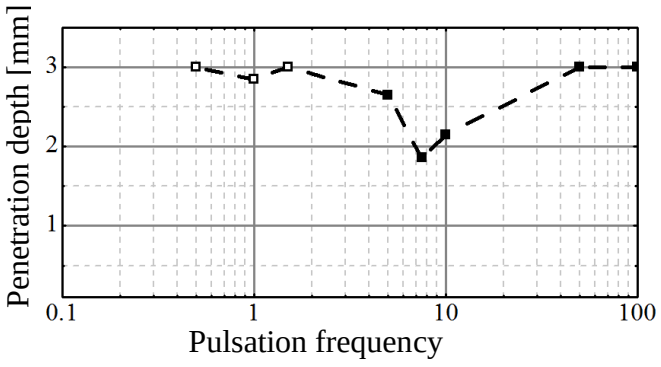

Fig. 5. Dependence of the penetration depth on the frequency of the pulsing current. White points indicate the variable depth of penetration for a given pulsation frequency

At the stage of macroscopic observations, there was a suspicion of the existence of significant chemical heterogeneities that may be the result of the crystallization process. One of the most common ways of controlling crystallization processes is the appropriate welding shape coefficient, i.e. the ratio between the width and depth of welding φ. However, different microstructures were obtained in samples 3, 4 and 7 with similar shape coefficients, which was confirmed in further studies presenting the results of microscopic tests and chemical analysis of micro-areas.

Using the relationship between the transverse field of the weld and the heat input (1) [13], the melting efficiency η 'obtained for the process realized with constant heat input but variable frequency was calculated.

$$A = \frac{\eta' \eta \cdot U \cdot I}{Q \cdot v} \tag{1}$$

where:
A – cross-section of the weld (mm²);
v – welding speed (mm/s);
Q – the theoretical amount of heat required to melt a unit volume of metal also called melting enthalpy, for steel Q = 10,5 J/mm³.
The thermal efficiency coefficient η according to PN EN 1011-1 was assumed to be 0.6. For the frequency of 0.5 Hz, the arithmetic mean was calculated from the values obtained for two different cross-sections taken within one cycle.

Two melting efficiency values were determined for each frequency, one based on the heat input calculated from the current and voltage effective values and the other from the average values. The obtained values represented in table V and on the graph (Fig. 6). When analyzing the calculated values, it should be taken into account that in the formula for melting efficiency, the cross-sectional area of welding is a representation of the volume of molten metal, so in the case of the first three samples, inaccuracies related to the measurement of melting efficiency should be considered. However, the inaccuracy in measuring the surface area is less important than the penetration depth.

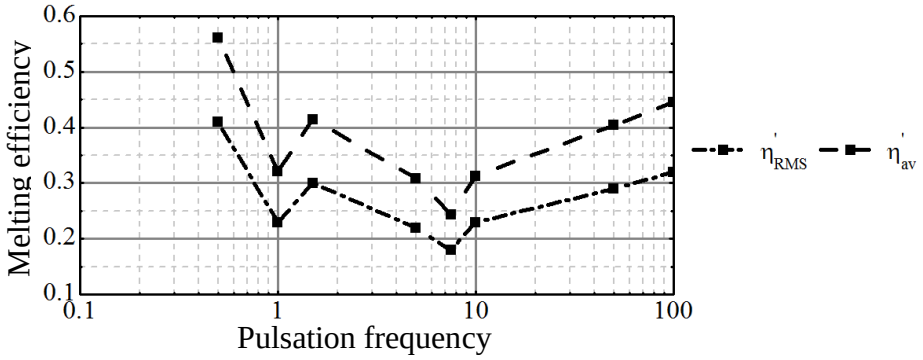

Fig. 6. Dependence of the melting efficiency on the frequency of the pulsating current

Table V. Comparison of melting efficiency values calculated using effective parameters (η'sk) and average current (η'śr) for welds performed at different pulse frequencies

f [Hz]	0.5	1	1,5	5	7,5	10	50	100
η' śr	0.56	0.32	0.41	0.31	0.24	0.31	0.40	0.45
η' sk	0.41	0.23	0.30	0.22	0.18	0.23	0.29	0.33

Fusion zone

Austenite dendrites arranged in different directions were visible in the welding microstructure in samples from 1 to 4. Ferrite was mainly found in skeletal and lamellar form, which results from local changes in the chemical composition, namely from the ratio of chromium to nickel equivalent. In the structure of samples from 1 to 6 it was possible to distinguish zones of overlapping successive thermal cycles. Observations of the samples showed the smallest dendritic structure in samples 3 and 4, welded at a pulse frequency of 1.5 and 5 Hz.

In samples 4 to 8, characteristic areas were observed, which could be the place of segregation of additives or impurities. In samples 4, 5 and 6 these areas were located in the upper part of the weld. The ferrite morphology in these samples was variable. Near the fusion line, ferrite occurred between the

austenite column crystals (interdendritic ferrite) (Fig. 7a), closer to the center took the form of skeletons and plates, and in the central part of the weld (Fig. 7b), an area of significant chemical heterogeneity was observed near the face (Fig. 7c).

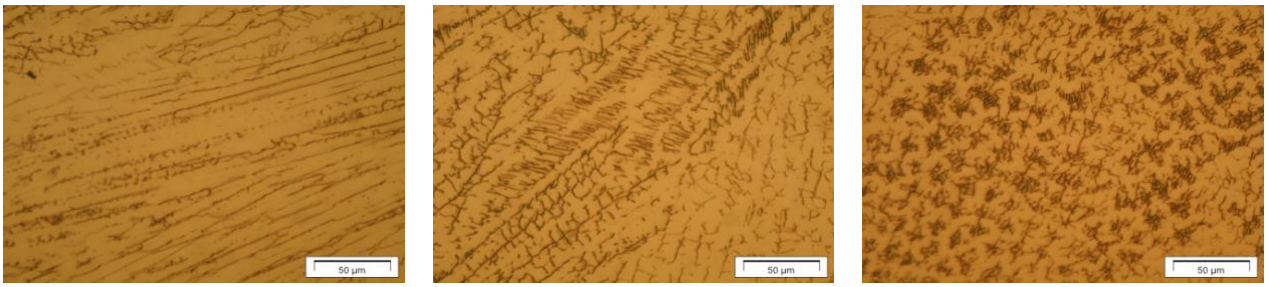

(a) area near the fusion line

(b) area between the fusion line and the central part of weld

(c) upper part at the center of the weld close to the face

Fig. 7. Microstructure in specimen 6 welded at 7.5 Hz. Picture a) ferrite in interdendritic spaces, b) skeletal and lamellar ferrite, c) segregation in the upper part of the weld

In samples 7 and 8 at the maximum penetration depth (full penetration), segregation took place in the welding axis at the junction of dendrites growing opposite each other. Areas with axial segregation were subjected to EDS chemical analysis and the presence of phosphorus up to 0.16% and an increase in carbon content was found. The results of spot microanalysis are shown in figure 8.

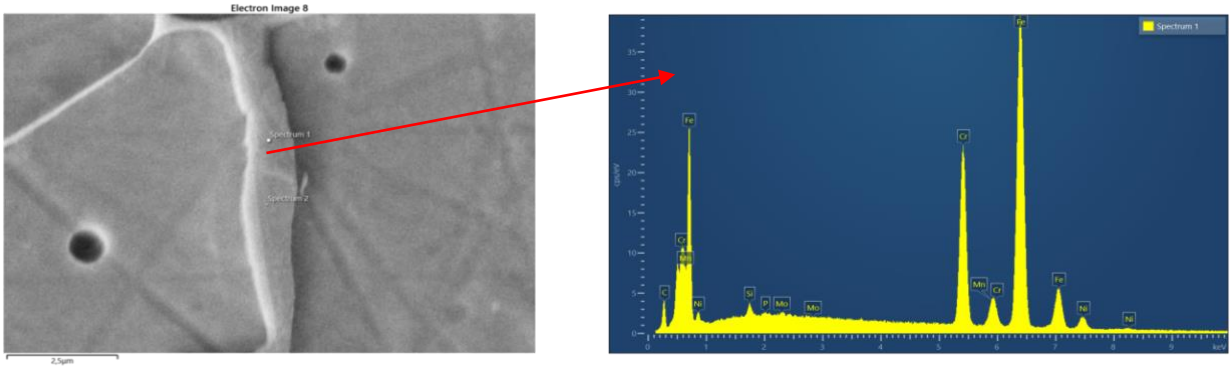

Statistics	C	Si	P	Cr	Mn	Fe	Ni	Mo
Max	4.91	0.50	0.16	22.01	1.73	66.36	4.38	0.40
Min	4.54	0.49	0.09	21.81	1.68	66.27	4.29	0.37
Average	4.73	0.50	0.13	21.91	1.70	66.32	4.33	0.39
Standard Deviation	0.26	0.01	0.05	0.14	0.03	0.06	0.06	0.03

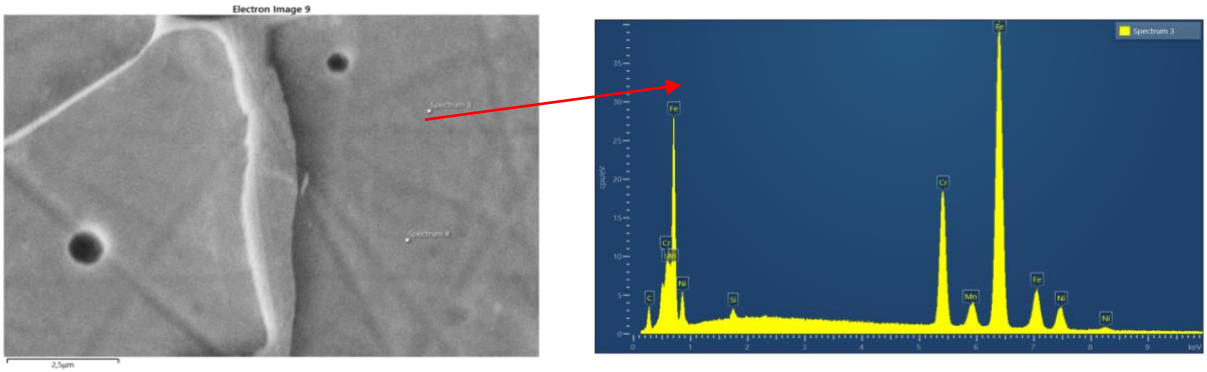

Statistics	C	Si	Cr	Mn	Fe	Ni
Max	4.14	0.43	17.50	2.05	67.50	8.79
Min	4.00	0.41	17.25	1.74	67.46	8.72
Average	4.07	0.42	17.38	1.90	67.48	8.76
Standard Deviation	0.10	0.01	0.18	0.22	0.03	0.05

Fig. 8. The spectrum of EDS in selected areas: on the top - the area with increased content of chromium and phosphorus, on the bottom - the area of the matrix with clearly raised level of nickel. Separate analyses were performed for each point

Heat affected zone

The heat affected zone microstructure examination showed the presence of ferrite stringers arranged in a direction parallel to the sample plane, i.e. in accordance with the rolling direction. In the structure, longer ferrite bands were observed, which extended deeper into the parent material, even above 500 μm. Rolling, causing deformation and hence strengthening the material, introduces high density of defects that increase its energy level. Partial melting, which is observed in single-phase alloys in segregation areas, can also take place in areas with increased internal energy, i.e. in bands according to the rolling direction (Fig. 9c).

In the fusion zone in most samples, residues after migration of austenite grain boundaries could be observed. In the "ghost" boundaries one can usually expect an increased concentration of additives [14,15] (Fig. 10). The migration of boundaries can be caused by phase transitions during cooling but during welding with pulsating current, they are caused by successive thermal cycles.

The general microstructure elements of the heat affected zone were similar for all tested samples. The main difference was in the width of the heat affected zone. Due to the fact that the welds had different depths, the width of the heat affected zone was measured in the middle of the welding height. The results of the measurements are presented in table VI.

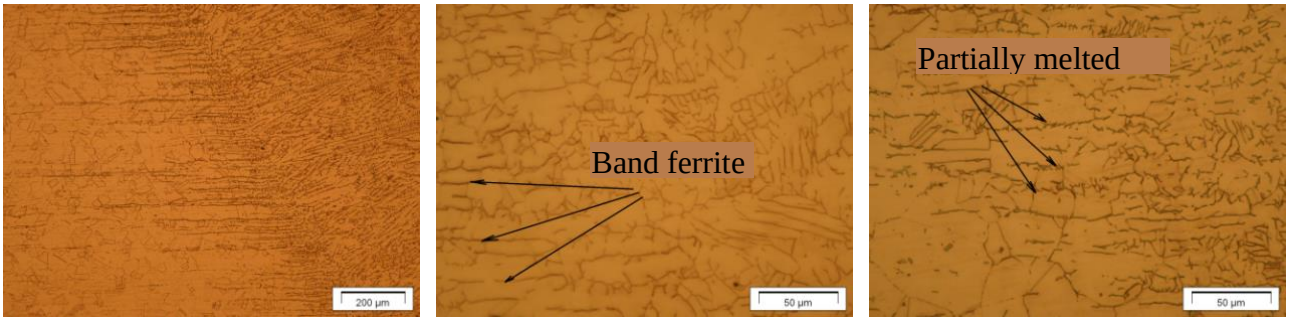

(a) (b) (c)

Fig. 9. Microstructure of the heat affected zone: a) long ferrite - δ stringers, b) partially fused area, c) fusion line

Table VI. Heat affected zone width in individual samples

Sample No.	1a	1b	2	3	4	5	6	7	8
HAZ width [μm]	180	260	325	385	455	160	120	540	565

The measurements of the width of the heat affected zone were related to the depth and cross-sectional area of the welding. No relationship was observed between these geometrical parameters, which may indicate a different amount of heat absorbed by the material. The lowest width of the heat affected zone was obtained for the sample welded at 10 Hz, while the lowest depth and welding transverse field was obtained for the sample welded at 5 Hz pulsation frequency.

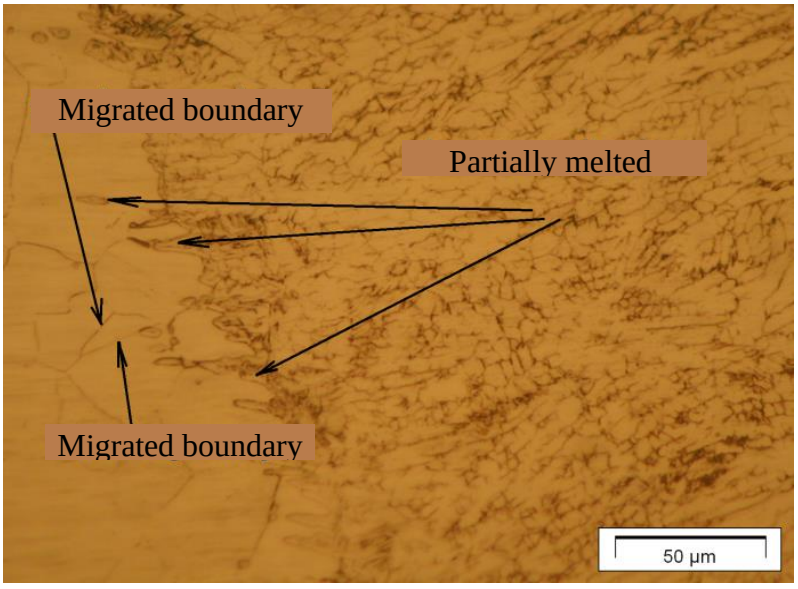

Fig. 10. Fusion line in the sample 1. Visible traces of migrating boundaries

During scanning microscope examinations in the fusion line, larger clusters of spherical precipitates were observed in samples 7 and 8. Chemical analysis of their composition showed the presence of manganese, silicon, oxygen and aluminum. These precipitations occurred in larger bands in the fusion zone (Fig. 11). In Almoussawi's study [16], it was found that a short, several-second heating time at a temperature of about 1500 °C can cause segregation of these elements in steel (the higher the temperature, the lower the segregation).

The samples also revealed the presence of a compound from the $CaO\text{-}Al_2O_3$ phase equilibrium system. This compound most likely originated from the steel deoxidation and desulphurization process [17], which consists in adding to the melted metal an alloy containing a component having a higher affinity for oxygen or sulfur than iron. In studies [16], coalescence of compounds of other elements (e.g. manganese, silicon, phosphorus and sulfur) was observed around $CaO\text{-}Al_2O_3$.

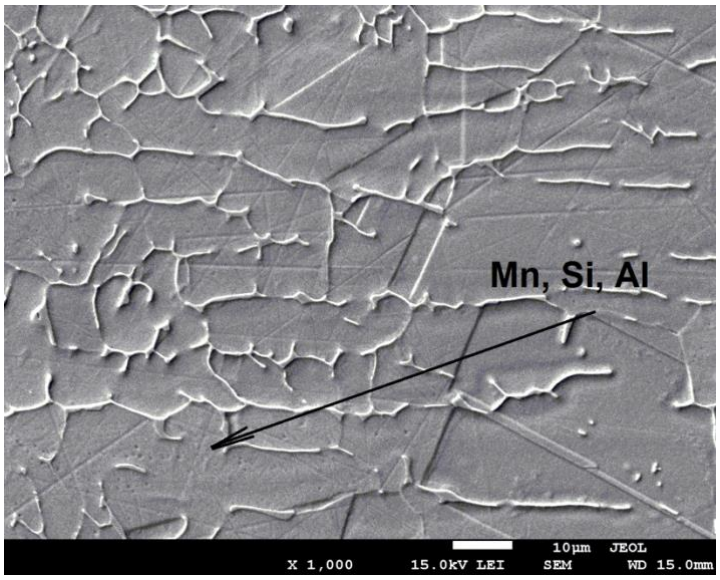

Fig. 11. Precipitations in the fusion line in the form of segregation bands in sample 8

Discussion of the results

The results obtained clearly show the impact of the current pulse frequency on the result of welding of 301L austenitic steel.

- Current frequencies affect the welding geometry and melting efficiency.
- Changes of the microstructure in the welds and in the heat affected zone observed during the tests indicate a definite dependence on the frequency. Such differences are usually associated with differences in the amount of heat introduced into the material, but the amount of heat input per unit of weld length, was constant and independent of the pulsation frequency for all performed processes.

The results of the research are difficult to compare with the other authors investigations, because research on the frequency of pulsating current, as the only variable process parameter, is not available in published papers. In addition, the results obtained for steel 321 in [7] indicate a high probability that the direction of changes obtained as part of the experiment may be different for each other configuration of welding parameters.

It should be noted that the results presented in the charts were not described by any regression relationship. Instead, the measuring points were connected, which was only to highlight the differences in the obtained welding results. These charts show a low frequency range (0.5÷1.5 Hz), where the cooling time is long enough that each subsequent pulse causes the melting of the area that has already crystallized again. For higher pulsation frequencies (from 5 Hz), the appearance of the weld indicates that the material remains in the liquid state between successive pulses. It can therefore be assumed that the mechanisms that affect the way heat propagates and shape the final appearance of the weld are frequency dependent. Some researchers [1] see a great similarity in welding in the higher frequency range for DC welding, what completely ignores the effect of varying arc pressure and welding pool vibration force. The impact of the variable heat cycle and increasing arc pressure was analyzed in [18÷20], while the resonance between arc pulsation and weld pool oscillation was investigated by Sorensen and Eagar as well as Xiao and Den Ouden [21÷24]. The research of these authors may form the basis for the interpretation of the results

obtained, and, taking into account the phenomena of wave nature, exclude the possibility of creating unambiguous relationships describing the impact of the frequency of pulsations on the depth of penetration or melting efficiency. The nature of the relationship shown in the graphs (Fig. 5 and Fig. 6) can also be associated with the changing properties of the material itself, dispersion, i.e. different heat absorption depending on the frequency of the energy transfer wave inside the material [25,26].

Another important issue is heat input, which depending on the calculation method could have different values. And because the value of heat input is related to mathematical relationships with melting efficiency, crystallization and cooling speed, maximum temperature values and the width of the heat affected zone, it is important to finally standardize its calculation method. This problem is well illustrated, e.g. by the possibility of obtaining different melting efficiency coefficients for the same process only due to computational controversies related to heat input (Fig. 6).

Apart from measuring and calculation aspects, the question arises: does the heat input really reflect the amount of heat input per unit length of the weld during the pulse process and is it a parameter that has a decisive influence on welding results? If we assume that it is so, then it would be expected that the result of welding performed at the same value of heat input would be the same. However, the results of the experiment carried out under constant heat input conditions show significant differences, which leads to the conclusion that the way of heat supply is at least as important as its quantity and affects the material's ability to absorb the heat.

It should also be noted that the research assumed a constant value of 0.6 as the process efficiency coefficient, while in the literature there are no calorimetric studies regarding the TIG process efficiency for pulsating current.

Conclusions

- The frequency of pulsations is an important factor influencing the results of TIG welding with pulsed current. The differences in welding results at different current frequencies are associated with the differences in the mechanism of forming the liquid pool.
- Heat input in the case of pulsed current TIG welding is not a helpful parameter in predicting welding results and should not be treated as a technological parameter.

Author Contributions: conceptualization M. O. and A. K.; methodology M. O.; research M. O.; writing – original draft preparation M.O.; writing – review and editing M. O.

Funding: Research statutory work of Warsaw University of Technology.

Conflicts of Interest: The authors declare no conflict of interest.

References

[1] Dzelnitzki D., Muendersbach, TIG Welding with High Frequency Pulses, an Interesting Process Variant. EWM Hightech Welding GmbH, 2000. [Hyperlink]

[2] Yang M., Yang Z., Cong, B. And Qi B., A Study on The Surface Depression Of The Molten Pool With Pulsed Welding. *Welding Journal*, 2014, Vol. 93, August 312-319. [CrossRef]

[3] Qi B., Yang M., Cong B., Li W., Study on Fastconvert Ultrasonic Frequency Pulse TIG welding Arc Characteristics. *Materials Science Forum* 2012, Vols. 704-705, 745-751. [CrossRef]

[4] Qi B.J., Yang M.X., Cong B.Q., Liu F. J. The effect of arc behavior on weld geometry by high-frequency pulse GTAW process with 0Cr18Ni9Ti stainless steel. *The International Journal of Advanced Manufacturing Technology* 2013, Vol. 66(9-12), 1545–1553. [CrossRef]

[5] Arivarasu M., Devendranath Ramkumar K., Arivazhagan N., Comparative Studies of High and Low Frequency Pulsing on the Aspect Ratio of Weld Bead in Gas Tungsten Arc Welded AISI 304L Plates. *Procedia Engineering*, 2014, Vol. 97, 871-880. [CrossRef]

[6] Traidia A., Multiphysics modeling and numerical simulation of GTA weld pools (Ph. Thesis - 2011) HAL Archives Ouvertes.fr. [Hyperlink]

[7] Ostromęcka M., Cegielski P., Kolasa A., Influence of pulse current frequency in the TIG method on selected aspects of heat supply during welding of 321 steel. *Welding Technology Review*, 2018, Vol. 90(3), 13-16. [CrossRef]

[8] Ugla A.A., A Comparative Study of Pulsed and Non-Pulsed Current on Aspect Ratio of Weld Bead and Microstructure Characteristics of AISI 304L Stainless Steel. *Innovative Systems Design and Engineering*, 2016, Vol. 7(4). [Hyperlink]

[9] Ugla A.A., Characterisation of Metallurgical and Mechanical Properties of the Welded AISI 304L Using Pulsed and Non-Pulsed Current TIG Welding International Journal of Chemical, Molecular, Nuclear. *Materials and Metallurgical Engineering*, 2016, Vol. 10(4). [CrossRef]

[10] Wojsyk K., Macherzyński M., Determination of Welding Linear Energy by Measuring Cross-Sectional Areas of Welds. *Biuletyn Instytutu Spawalnictwa,* 2016, Vol. 60(5), 83-89. [CrossRef]
[11] Wojsyk K., Macherzyński M., Lis R., Evaluation of the amount of heat introduced into the welds and padding welds by means of their transverse fields measurement in conventional and hybrid welding processes. *Welding Technology Review,* 2017, Vol. 89(10), 67-82. [CorssRef]
[12] Cegielski P., Bugyi Ł., Selected aspects of welding defects identification in MIG/MAG arc welding. *Welding Technology Review*, 2017, Vol. 89(6), 30-35. [CorssRef]
[13] Klimpel A., Technology of welding and cutting. Publishing House of Silesian University of Technology, Gliwice 1997.
[14] Arivarasu M., Kasinath D.R., Natarajan A., Effect of Continuous and Pulsed Current on the Metallurgical and Mechanical Properties of Gas Tungsten Arc Welded AISI 4340 Aeronautical and AISI 304L Austenitic Stainless Steel Dissimilar Joints. *Materials Research*, 2015, 18(I), 59-77. [CorssRef]
[15] Tasak E., Metallurgy of Welding, Cracow 2008.
[16] Almoussawi M., Smith A., Faraji M., Carter S., Segregation of Mn, Si, Al and oxygen during friction stir welding of DH36 Steel. *Metallography, Microstructure, and Analysis*, 2017, Vol. 6(6), 569-576. [CorssRef]
[17] Lind M., Mechanism and Kinetics of Transformation of Alumina Inclusions In Steel By Calcium Treatment, Doctoral thesis, Helsinki University of technology, 2006.
[18] Eagar T.W., The Physics of Arc Welding Processes. *Advanced Joining Technologies*, 1990. [CorssRef]
[19] Lancaster J.F., The Physics of Welding, Pergamon Press, 1984.
[20] Lin M.L., Eagar T.W., Pressures Produced by Gas Tungsten Arcs, *Metallurgical Transactions B*, 1986, Vol. 17B(3). [CorssRef]
[21] Sorensen C.D., Eagar T.W., Measurement of oscillations in partially penetrated weld pools through spectral analysis'. *J. Dyn. Syst. Meas. Contr.,* 1990, Vol. 112(3), 463-468. [CorssRef]
[22] Sorensen C.D., Eagar T.W., Modeling of oscillations in partially penetrated weld pools'. *J. Dyn. Syst. Meas. Contr.* 1990, Vol. 112(3), 469–474. [CorssRef]
[23] Xiao Y.H., Den Ouden G., A study of GTA weld pool oscillation. *Welding Research Supplement*, 1990, 69, 289-293. [Hyperlink]
[24] Xiao Y.H., Den Ouden G., Weld pool oscillation during GTA welding of mild steel. *Welding Research Supplement*, 1993, 72, 428-434. [Hyperlink]
[25] Ostromęcka M., Influence of the frequency of pulsating TIG welding current on the effects of heat in selected special steels. Doctoral thesis, Warsaw University of Technology, 2019.
[26] Karpierz M., Basics of photonics. CSZ Warsaw University of Technology, Warsaw 2010.